Journal of
Materials Chemistry

Cite this: *J. Mater. Chem.*, 2012, **22**, 10537

www.rsc.org/materials

PAPER

Fluorenobenzofuran as the core structure of high triplet energy host materials for green phosphorescent organic light-emitting diodes

Soon Ok Jeon and Jun Yeob Lee*

Received 24th January 2012, Accepted 20th March 2012
DOI: 10.1039/c2jm30473b

Thermally stable high triplet energy host materials based on a fluorenobenzofuran (BFF) core were synthesized and the device performances of green phosphorescent organic light-emitting diodes were investigated. BFF was designed as the electron transport type core with improved thermal stability. Two host materials based on the BFF core showed a high glass transition temperature over 140 °C and high triplet energy above 2.70 eV. They were used as the host materials for green phosphorescent organic light-emitting diodes and a high quantum efficiency close to 20% was achieved.

Introduction

It is important to improve the quantum efficiency and lifetime of phosphorescent organic light-emitting diodes (PHOLEDs) by developing new emitting materials such as host and dopant materials. In particular, the host materials are critical to the device performances of PHOLEDs and various host materials have been synthesized.[1–16]

There are several requirements for the host materials in PHOLEDs, which include high triplet energy, high glass transition temperature, and highest occupied molecular orbital (HOMO)/lowest unoccupied molecular orbital (LUMO) levels for hole and electron injection. Several classes of materials have been reported and one of the most popular core structures to meet the requirements of host materials for PHOLEDs was fluorene.[17–26] The fluorene core structure shows a high triplet energy of 2.90 eV and weak electron transport properties. In addition, it can be chemically modified at 9,9′-position or 2,7-position of fluorene to tailor the physical and thermal properties with ease. Various functional groups such as diphenylamine,[18] diphenylphosphine oxide[19] and carbazole[17] were introduced in the molecular structure to control the charge transport properties of the fluorene based organic compounds. However, the simple chemical modification of the fluorene core could not improve the glass transition temperature and it was difficult to obtain bipolar charge transport properties due to weak electron transport properties of the fluorene core. Therefore, a new core structure with better electron transport properties and thermal stability is required to develop bipolar host materials with high glass transition temperature.

In this work, a thermally stable high triplet energy core structure, benzofuran modified flourene (BFF), was developed as a new core structure for bipolar host materials of PHOLEDs. The BFF was effectively synthesized by the ring closing reaction of the phenyl modified dibenzofuran and was modified with a hole transport type carbazole unit. It was demonstrated that the BFF based host materials showed a high triplet energy of 2.70 eV, high glass transition temperature above 140 °C, bipolar charge transport properties and over 19.0% external quantum efficiency in green PHOLEDs.

Experimental section

Synthesis

The synthetic scheme of the BFF based compounds is described in Scheme 1.

Synthesis of 4-(2-bromophenyl)dibenzo[*b*,*d*]furan (1). 4-Dibenzofuranylboronic acid (5.00 g, 23.58 mmol), 1,2-dibromobenzene (5.05 g, 21.43 mmol) and tetrakis(triphenylphosphine)palladium (1.23 g, 1.07 mmol) were dissolved in anhydrous tetrahydrofuran (THF) under nitrogen atmosphere. The reaction mixture was stirred for 1 h. To the reaction mixture was added a solution of potassium carbonate (2 M, 50 mL) dropwise slowly. The reaction mixture was refluxed for 12 h at 90 °C under nitrogen

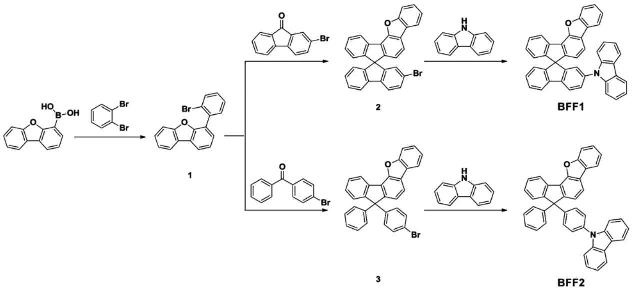

Scheme 1 Synthetic scheme of **BFF1** and **BFF2**.

Department of Polymer Science and Engineering, Dankook University, 126, Jukjeon-dong, Suji-gu, Yongin, Gyeonggi, 448-701, Republic of Korea. E-mail: leej17@dankook.ac.kr; Fax: +82 31 8005 3585; Tel: +82 31 8005 3585

atmosphere. After being cooled to ambient temperature, the reaction mixture was extracted with dichloromethane and water. The organic layer was evaporated with a rotary evaporator. The residue was subjected to column chromatography (silica gel) by *n*-hexane and a white powdery product was obtained.

Yield 86%. ^{1}H NMR (500 MHz, $CDCl_3$): δ 7.99 (d, 2H, J = 6 Hz), 7.77 (d, 1H, J = 8.0 Hz), 7.53–7.32 (m, 8H). ^{13}C NMR (125 MHz, $CDCl_3$) δ 156.4, 137.8, 133.8, 132.7, 131.6, 130.2, 129.1, 128.1, 126.9, 125.6, 124.6, 123.9, 123.5, 122.5, 121.5, 120.4, 112.6, 111.6. MS (FAB) *m*/*z* 323 [(M + H)$^+$]. Anal. calcd for $C_{18}H_{11}BrO$: C, 66.89; H, 3.43. Found: C, 66.88; H, 3.44%.

Synthesis of 2-bromospiro[fluorene-9,7′-fluoreno[4,3-*b*]benzofuran] (2). 4-(2-Bromophenyl)dibenzo[*b*,*d*]furan (**1**) (3.00 g, 9.28 mmol) was dissolved in 30 mL of anhydrous tetrahydrofuran under argon and cooled to −78 °C and *n*-butyllithium (2.5 M in hexanes, 4.83 mL) was added dropwise slowly. Stirring was continued for 2 h at −78 °C, followed by the addition of a solution of 2-bromofluorenone (3.12 g, 12.06 mmol) in THF (40 mL) under an argon atmosphere. The resulting mixture was gradually warmed to ambient temperature and quenched by adding saturated, aqueous $NaHCO_3$ (100 mL). The mixture was extracted with dichloromethane. The combined organic layers were dried over magnesium sulfate, filtered, and evaporated under reduced pressure. A yellow powdery product was obtained. The crude residue was placed in another two-necked flask and was dissolved in acetic acid (40 mL). A catalytic amount of aqueous HCl (5 mol%, 12 N) was then added and the whole solution was refluxed for 12 h. After cooling to ambient temperature, purification by silica gel chromatography using dichloromethane–*n*-hexane (1 : 4) gave a white powder.

Yield 69%. ^{1}H NMR (500 MHz, $CDCl_3$): δ 8.38 (d, 1H, J = 8.0 Hz), 7.95 (d, 1H, J = 8.0 Hz), 7.89–7.82 (m, 1H), 7.77–7.67 (m, 3H), 7.51–7.35 (m, 5H), 7.19–7.08 (m, 2H), 6.87–6.69 (m, 4H). ^{13}C NMR (125 MHz, $CDCl_3$) δ 156.8, 150.6, 148.3, 147.9, 147.6, 140.7, 139.3, 131.0, 128.3, 127.8, 127.1, 124.6, 124.2, 123.8, 123.3, 123.0, 121.5, 121.3, 120.5, 120.1, 119.8, 118.4, 111.9, 66.61. MS (FAB) *m*/*z* 485 [(M + H)$^+$]. Anal. calcd for $C_{31}H_{17}BrO$: C, 76.71; H, 3.53. Found: C, 75.83; H, 3.46%.

Synthesis of 7-(4-bromophenyl)-7-phenyl-7*H*-fluoreno[4,3-*b*] benzofuran (3). This compound was prepared by a procedure similar to that of (**2**) except 4-bromobenzophenone that was used as the reactant instead of 2-bromofluorenone. The product was purified by column chromatography using dichloromethane–*n*-hexane (1 : 4) which gave a white powder.

Yield 77%. ^{1}H NMR (500 MHz, $CDCl_3$): δ 8.33 (d, 1H, J = 8.0 Hz), 7.96 (d, 1H, J = 8.0 Hz), 7.85 (d, 1H, J = 8.0 Hz), 7.70 (d, 1H, J = 8.0 Hz), 7.53–7.33 (m, 13H), 7.13–7.09 (m, 2H). ^{13}C NMR (125 MHz, $CDCl_3$) δ 156.3, 150.3, 149.8, 144.4, 137.2, 131.3, 130.3, 129.9, 129.0, 128.3, 127.7, 127.0, 125.7, 124.7, 123.7, 123.0, 122.4, 122.0, 120.4, 119.5, 118.7, 111.9, 110.8, 65.4. MS (FAB) *m*/*z* 487 [(M + H)$^+$]. Anal. calcd for $C_{31}H_{19}BrO$: C, 76.39; H, 3.93. Found: C, 76.42; H, 3.94%.

Synthesis of 9-(spiro[fluorene-9,7′-fluoreno[4,3-*b*]benzofuran]-2-yl)-9*H*-carbazole (BFF1). 2-Bromospiro[fluorene-9,7′-fluoreno[4,3-*b*]benzofuran] (**2**) (2.00 g, 4.12 mmol), 9-carbazole (0.83 g, 4.94 mmol), copper powder (0.52 g, 8.24 mmol), dibenzo 18-crown-6 (0.11 g, 0.41 mmol) and potassium carbonate (2.28 g, 16.48 mmol) were dissolved in anhydrous *o*-dichlorobenzene under nitrogen atmosphere. The reaction mixture was stirred for 12 h at 120 °C. The mixture was diluted with dichloromethane and washed with distilled water (100 mL) three times. The organic layer was dried over anhydrous $MgSO_4$ and evaporated *in vacuo* to give the crude product, which was purified by column chromatography by *n*-hexane–dichloromethane (4 : 1). The final white powdery product was obtained in 68% yield.

BFF1 Yield 68%. T_g 146.9 °C. ^{1}H NMR (500 MHz, $CDCl_3$): δ 8.33 (d, 1H, J = 7.6 Hz), 8.10–7.93 (m, 6H), 7.73 (t, 2H, J = 7.9 Hz), 7.61–7.36 (m, 6H), 7.30–7.13 (m, 6H), 6.94–6.79 (m, 4H). ^{13}C-NMR (125 MHz, $CDCl_3$) δ 170.6, 156.2, 150.1, 148.3, 147.6, 140.4, 139.9, 138.8, 128.2, 127.2, 125.8, 124.7, 124.0, 123.6, 122.7, 121.7, 121.1, 120.5, 120.2, 119.8, 118.9, 118.7, 117.3, 112.0, 109.6, 108.5, 66.9. MS (FAB) *m*/*z* 571 [(M + H)$^+$]. Anal. calcd for $C_{43}H_{24}NO$: C, 90.34; H, 4.41; N, 2.45. Found: C, 90.26; H, 4.56; N, 2.47%.

Synthesis of 9-(4-(7-phenyl-7*H*-fluoreno[4,3-*b*]benzofuran-7-yl) phenyl)-9*H*-carbazole (BFF2). This compound was prepared by a procedure similar to that of **BFF1** except that 7-(4-bromophenyl)-7-phenyl-7*H*-fluoreno[4,3-*b*]benzofuran (**3**) was used as the reactant instead of 2-bromospiro[fluorene-9,7’-fluoreno[4,3-*b*]benzofuran] (**2**). Purification by column chromatography using *n*-hexane–dichloromethane (4 : 1) gave a white powder.

BFF2 Yield 68%. ^{1}H NMR (500 MHz, $CDCl_3$): δ 8.33 (d, 1H, J = 7.6 Hz), 8.10–7.93 (m, 6H), 7.73 (t, 2H, J = 7.9 Hz), 7.61–7.36 (m, 7H), 7.30–7.13 (m, 6H), 6.94–6.79 (m, 4H). ^{13}C NMR (125 MHz, $CDCl_3$): δ 157.2, 151.5, 150.9, 145.6, 145.1, 140.9, 138.1, 136.6, 130.4, 129.2, 128.9, 127.9, 127.5, 126.6, 125.5, 124.3, 123.6, 121.4, 121.1, 120.5, 119.9, 119.6, 112.7, 111.5, 110.6, 109.5, 67.7. MS (FAB) *m*/*z* 573 [(M + H)$^+$]. Anal. calcd for $C_{43}H_{27}NO$: C, 90.03; H, 4.74; N, 2.44. Found: C, 90.02; H, 4.73; N, 2.34%.

Device preparation and measurements

The device structure of green PHOLEDs was indium tin oxide (ITO, 50 nm)/*N*,*N*′-diphenyl-*N*,*N*′-bis-[4-(phenyl-*m*-tolyl-amino)-phenyl]-biphenyl-4,4′-diamine (DNTPD, 60 nm)/4,4′-(cyclohexane-1,1-diyl)bis(*N*-phenyl-*N*-*p*-tolylaniline) (TAPC, 30 nm)/**BFF1** or **BFF2**:tris(2-phenylpyridine) iridium ($Ir(ppy)_3$) (30 nm, 3%)/diphenylphosphine oxide-4-(triphenylsilyl)phenyl (TSPO1, 25 nm)/LiF (1 nm)/Al (200 nm). A hole only device with a device structure of ITO (50 nm)/DNTPD (60 nm)/TAPC (30 nm)/**BFF1** or **BFF2** (30 nm)/Al and an electron only device with a device structure of ITO (50 nm)/Ca (5 nm)/**BFF1** or **BFF2** (30 nm)/TSPO1 (25 nm)/LiF (1 nm)/Al (200 nm) were also fabricated. The device performances of green PHOLEDs were measured with a Keithley 2400 source measurement unit and CS1000 spectroradiometer after encapsulating the device with a glass lid and CaO getter.

The ^{1}H and ^{13}C nuclear magnetic resonance (NMR) was recorded on a Varian 500 (500 MHz) spectrometer. The photoluminescence (PL) spectra were recorded on a fluorescence spectrophotometer (HITACHI, F-7000) and the ultraviolet-visible (UV-Vis) spectra were obtained using a UV-Vis spectrophotometer (Shimadzu, UV-2501PC). The differential scanning calorimeter (DSC) measurements were performed on a Mettler

DSC 822e under nitrogen at a heating rate of 10 °C min^{-1}. The low and high resolution mass spectra were recorded using a JEOL, JMS-AX505WA spectrometer in FAB mode. The energy levels were measured by cyclic voltammetry (CV).

Results and discussion

Two BFF based host materials, **BFF1** and **BFF2**, were developed as thermally stable bipolar host materials for balanced hole and electron density in the emitting layer. The BFF core was designed as the electron transport type core structure with high triplet energy and high rigidity for high glass transition temperature. The benzofuran unit withdraws electrons due to the oxygen with high electronegativity, making the fluorene electron deficient. Therefore, the BFF core can function as the electron transport type core structure. In addition to the electron transport properties, the BFF may improve the glass transition temperature because the molecular motion of the benzofuran unit is restricted by the fluorene unit. The BFF core may have high triplet energy as the phenyl unit in the fluorene is attached to the *ortho*-position of the oxygen in the benzofuran and *meta*-position of the phenyl in the benzofuran. The extension of the conjugation is limited by the *ortho*- and *meta*-connection between the fluorene and benzofuran, resulting in wide bandgap and high triplet energy. As the BFF core was synthesized as the electron deficient core, it was modified with a hole transport type carbazole unit to obtain bipolar charge transport properties.

The BFF core could be synthesized by the coupling reaction between 4-dibenzofuranylboronic acid and 1,2-dibromobenzene followed by the ring closing reaction with 4-bromobenzophenone or 2-bromofluorenone. The synthetic yield of the brominated BFF cores was in the range from 69% to 77%. The brominated intermediates were reacted with carbazole using copper powder as the catalyst. The synthetic yield of **BFF1** and **BFF2** from brominated BFF cores was 68% for both compounds.

Molecular simulation of **BFF1** and **BFF2** was carried out to study the highest occupied molecular orbital (HOMO) and the lowest unoccupied molecular orbital (LUMO) distribution of the host materials. A suite of the Gaussian 03 program and the nonlocal density functional of Becke's 3-parameters employing the Lee–Yang–Parr functional (B3LYP) with 6-31G* basis sets were used for the simulation.[27] Fig. 1 shows the HOMO and LUMO distribution of **BFF1** and **BFF2**. The HOMO and LUMO distribution of **BFF1** and **BFF2** was quite similar. The HOMO was localized on the 9-phenylcarbazole unit, while the LUMO was dispersed over the BFF core. As can be expected from the molecular structure, the HOMO and LUMO were distributed over the electron donating 9-phenylcarbazole unit and electron withdrawing BFF core unit, respectively. This indicates that the HOMO of **BFF1** and **BFF2** is decided by the carbazole, while the LUMO is determined by the BFF core.

Photophysical properties of **BFF1** and **BFF2** were measured using UV-Vis and PL spectrometers. Fig. 2 represents the UV-Vis and PL spectra of **BFF1** and **BFF2**. Both host materials showed similar UV-Vis and PL spectra although slight red-shift of the spectra was observed in **BFF1**. The UV-Vis absorption peaks at 293 nm, 323 nm and 340 nm are assigned to π–π* transition of phenylcarbazole, while peaks at 276 nm and 308 nm correspond to π–π* transition of the BFF core. The conjugation of the phenylcarbazole is extended through the fluorene unit in **BFF1**, slightly shifting the UV-Vis absorption peak to long wavelength. Bandgaps of the **BFF1** and **BFF2** were calculated from the edge of the UV-Vis absorption spectra, which were 3.53 eV and 3.55 eV, respectively. The extended conjugation of the **BFF1** slightly reduced the bandgap from 3.55 eV to 3.53 eV. The PL emission was also shifted by 4 nm due to the extended conjugation between fluorene and carbazole in **BFF1**. There was little solvatochromic effect in both **BFF1** and **BFF2**, indicating weak charge transfer in host materials. Low temperature PL measurement was also carried out at 77 K in liquid nitrogen to

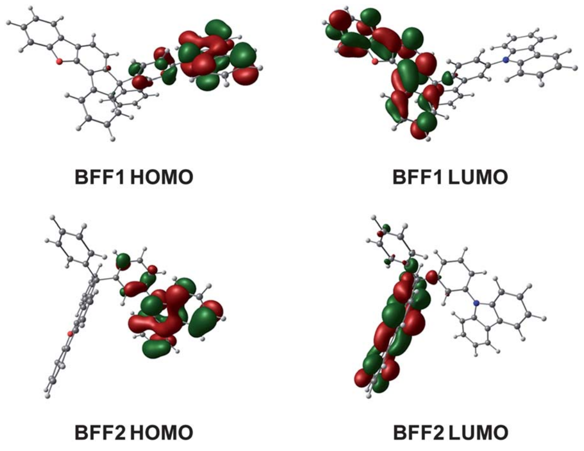

Fig. 1 HOMO and LUMO distribution of **BFF1** and **BFF2**.

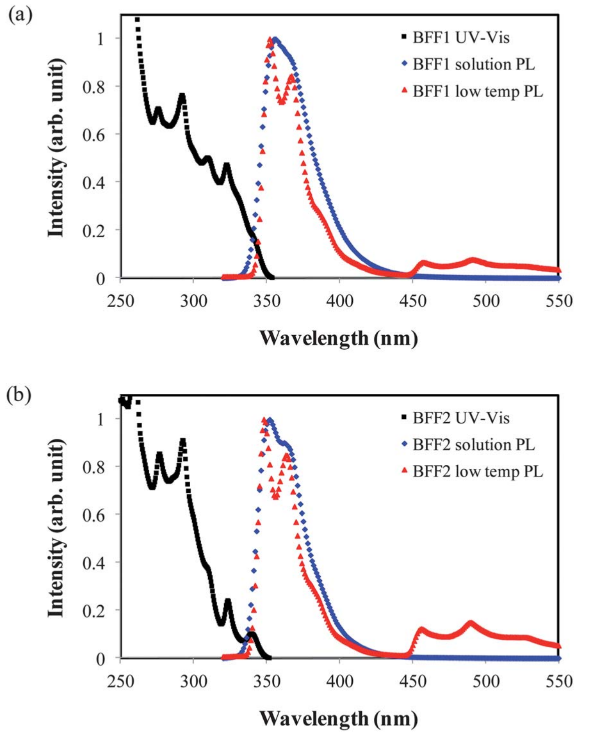

Fig. 2 UV-Vis, solution PL and low temperature PL spectra of (a) **BFF1** and (b) **BFF2**. UV-Vis and solution PL spectra were measured in tetrahydrofuran. Low temperature PL was obtained in liquid nitrogen.

measure the triplet energy of the host materials. The triplet energies were calculated from the first emission peak of low temperature PL spectra, which were 2.70 eV and 2.71 eV for **BFF1** and **BFF2**, respectively. The triplet energies of the host materials were high enough for energy transfer to green emitting Ir(ppy)$_3$ with a triplet energy of 2.4 eV.

Thermal transition of host materials was analyzed using DSC at a heating rate of 10 °C min^{-1} in nitrogen atmosphere. No melting transition was observed in **BFF1** and **BFF2** up to 400 °C and only glass transition was detected in **BFF1**. The glass transition temperature of the **BFF1** was 147 °C, which is higher than that of common spirobifluorene based host materials.[18,19] Therefore, the BFF core was effective to improve the glass transition temperature of host materials. The high glass transition temperature of **BFF1** is due to the rigidity of the BFF core structure.

The HOMOs of **BFF1** and **BFF2** were obtained by CV measurement, which were −6.06 eV and −6.09 eV from the onset of the oxidation peak (Fig. 3). Two host materials showed similar HOMO levels because the HOMO is dispersed over the phenylcarbazole unit in both compounds. The slight change of the HOMO level is due to the different conjugation of the phenylcarbazole unit. The LUMO was calculated from the HOMO and bandgap. The LUMOs of **BFF1** and **BFF2** were −2.53 eV and −2.54 eV, respectively. As the LUMO was localized on the same BFF core in the two host materials, there was little difference of LUMO level.

Hole only and electron only devices of **BFF1** and **BFF2** were fabricated to compare the charge transport properties of **BFF1** and **BFF2**. Current density–voltage curves of hole only and electron only devices are shown in Fig. 4. The current density of the hole only device was similar in **BFF1** and **BFF2**, while that of the electron only device was high in **BFF1**. Comparing the hole and electron current densities of **BFF1**, the hole current density was similar to electron current density, indicating bipolar charge transport properties of **BFF1**. However, the hole current density of **BFF2** was much higher than the electron current density of **BFF2**. Although both **BFF1** and **BFF2** were designed as the bipolar host materials, **BFF1** was more suitable as the bipolar host material. The high electron current density of **BFF1** may be due to the fluorene unit connected to the carbazole unit. As fluorene is a weak electron transport unit, the additional fluorene unit attached to the carbazole of **BFF1** facilitates electron transport of **BFF1** compared with **BFF2** without additional fluorene unit.

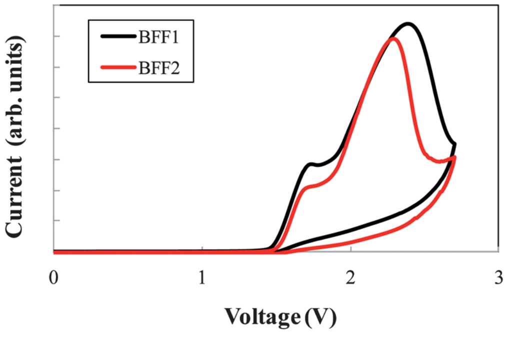

Fig. 3 Oxidation CV curves of **BFF1** and **BFF2**.

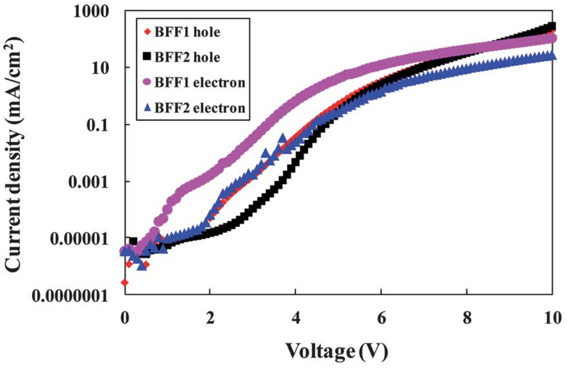

Fig. 4 Current density–voltage curves of hole only and electron only devices of **BFF1** and **BFF2**.

Green PHOLEDs doped with Ir(ppy)$_3$ were fabricated to evaluate **BFF1** and **BFF2** as the host materials. The doping concentration of Ir(ppy)$_3$ was 3%. Fig. 5 shows the current density–voltage–luminance curves of green PHOLEDs with **BFF1** and **BFF2** host materials. The current density of the **BFF1** device was higher than that of the **BFF2** device over all the voltage range measured. Considering the hole only and electron only device data, the high current density of the **BFF1** device is due to high electron density of the **BFF1** emitting layer. Although the hole current density of **BFF1** was lower than that of **BFF2**, the high electron current density increased the total current density of the **BFF1** device. The same trend was observed in the luminance–voltage curves of green PHOLEDs.

Quantum efficiency–luminance curves of green PHOLEDs with **BFF1** and **BFF2** host materials are shown in Fig. 6. The external quantum efficiency of the **BFF1** device was higher than that of the **BFF2** device over all the luminance range. The maximum external quantum efficiency of the **BFF1** device was 19.7% and the quantum efficiency at 1000 cd m^{-2} was 19.5%. In particular, the quantum efficiency at 5000 cd m^{-2} was also 18.3%. There was less than 10% decrease of quantum efficiency up to 5000 cd m^{-2}. However, the quantum efficiency of the **BFF2** device was greatly reduced at high luminance. The maximum quantum efficiency of the **BFF2** device was 18.6%, but the quantum efficiency at 5000 cd m^{-2} was only 11.5%. The difference of quantum efficiency between **BFF1** and **BFF2** devices can be explained by the hole and electron current densities in the

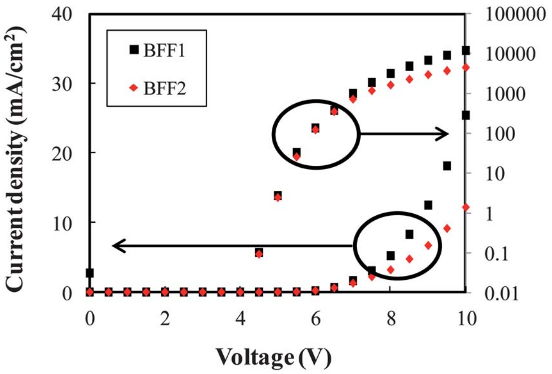

Fig. 5 Current density–voltage–luminance curves of **BFF1** and **BFF2** green PHOLEDs. Ir(ppy)$_3$ was doped at a doping concentration of 3%.

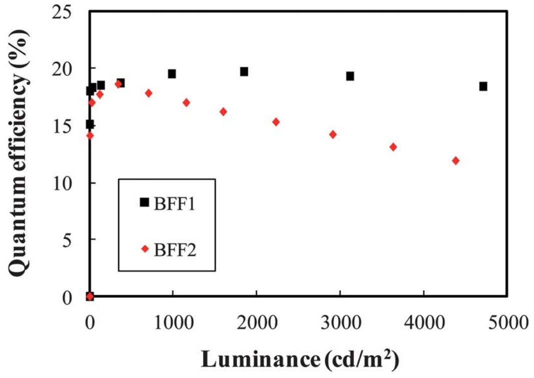

Fig. 6 Quantum efficiency–luminance curves of **BFF1** and **BFF2** green PHOLEDs.

Table 1 Device performances of **BFF1** and **BFF2** green devices

	Maximum quantum efficiency [%]	Quantum efficiency[a] [%]	Color index[b]	Maximum current efficiency [cd A^{-1}]	Maximum power efficiency [lm W^{-1}]
BFF1	19.7	19.5	(0.32,0.61)	60.5	38.8
BFF2	18.6	17.3	(0.33,0.61)	57.3	32.2

[a] Quantum efficiency was measured at 1000 cd m^{-2}. [b] Color index was measured at 1000 cd m^{-2}.

emitting layer. As shown in the hole and electron only device data, **BFF1** showed similar hole and electron density. The balanced charge density in the emitting layer enhances the quantum efficiency of the **BFF1** device and maintains the charge balance up to high luminance. However, the charge balance is disrupted in the **BFF2** device because of imbalance of charge density. Especially, the hole current density is much higher than the electron current density at high voltage, resulting in significant reduction of quantum efficiency at high luminance. All device performances of **BFF1** and **BFF2** are summarized in Table 1.

BFF1 and **BFF2** were evaluated as host materials for blue PHOLEDs, but the quantum efficiency was very low due to poor energy transfer. A quantum efficiency of 9.2% was obtained in red PHOLEDs.

Conclusions

In conclusion, thermally stable high triplet energy host materials, **BFF1** and **BFF2**, were synthesized using a fluorenobenzofuran core and were effectively used as the bipolar host materials for green PHOLEDs. **BFF1** showed a high glass transition temperature above 140 °C and a high triplet energy of 2.70 eV. In addition, a high external quantum efficiency of 19.7% was obtained from the green PHOLED with a **BFF1** host and less than 10% decrease of quantum efficiency was achieved up to 5000 cd m^{-2}. Therefore, the new fluorenobenzofuran can be useful as the core structure of thermally stable high triplet energy host and charge transport materials.

Notes and references

1 S.-J. Su, H. Sasabe, T. Takeda and J. Kido, *Chem. Mater.*, 2008, **20**, 1691.
2 R. J. Holmes, B. W. D. Andrade, S. R. Forrest, X. Ren, J. Li and M. E. Thompson, *Appl. Phys. Lett.*, 2003, **83**, 3818.
3 M. H. Tsai, H. W. Lin, H. C. Su, T. H. Ke, C. C. Wu, F. C. Tang, Y. L. Liao, K. T. Wong and C. I. Wu, *Adv. Mater.*, 2006, **18**, 1216.
4 M. F. Wu, S. J. Yeh, C. T. Chen, H. Murayama, T. Tsuboi, W. Li, I. Chao, S. Liu and J. K. Wang, *Adv. Funct. Mater.*, 2007, **17**, 1887.
5 X. Ren, J. Li, R. J. Holmes, P. I. Djurovich, S. R. Forrest and M. E. Thompson, *Chem. Mater.*, 2004, **16**, 4743.
6 Y. Tao, Q. Wang, L. Ao, C. Zhong, C. Yang, J. Qin and D. Ma, *J. Phys. Chem. C*, 2010, **114**, 601.
7 M. M. Rothmann, S. Haneder, E. D. Como, C. Lennartz, C. Schildknecht and P. Strohriegl, *Chem. Mater.*, 2010, **22**, 2403.
8 K. Son, M. Yahiro, M. T. Imai, H. Yoshizaki and C. Adachi, *Chem. Mater.*, 2008, **20**, 4439.
9 Y. Tao, Q. Wang, Y. Shang, C. Yang, L. Ao, J. Qin, D. Ma and Z. Shuai, *Chem. Commun.*, 2009, 77.
10 Y. Tao, Q. wang, C. Yang, Q. Wang, Z. Zhang, T. Zou, J. Qin and D. Ma, *Angew. Chem., Int. Ed.*, 2008, **47**, 8104.
11 M. K. Kim, J. Kwon, T.-H. Kwon and J.-I. Hong, *New J. Chem.*, 2010, **34**, 1317.
12 S. O. Jeon, K. S. Yook, C. W. Joo and J. Y. Lee, *Adv. Funct. Mater.*, 2009, **19**, 3644.
13 A. B. Padmaperuma, L. S. Sapochak and P. E. Burrows, *Chem. Mater.*, 2006, **18**, 2389.
14 S. O. Jeon, S. E. Jang, H. S. Son and J. Y. Lee, *Adv. Mater.*, 2011, **23**, 1436.
15 Y. Tao, C. Yang and J. Qin, *Chem. Soc. Rev.*, 2011, **40**, 2943.
16 A. Chaskar, H. Chen and K. Wong, *Adv. Mater.*, 2011, **23**, 3876.
17 P. Shih, C. Chiang, A. K. Dixit, C. Chen, M. Yuan, R. Lee, C. Chen, E. W. Diau and C. Shu, *Org. Lett.*, 2006, **8**, 2799.
18 P. Shih, C. Chien, F. Wu and C. Shu, *Adv. Funct. Mater.*, 2007, **17**, 2346.
19 S. E. Jang, C. W. Jang, S. O. Jeon, K. S. Yook and J. Y. Lee, *Org. Electron.*, 2010, **11**, 1059.
20 T. Spehr, R. Pudzich, T. Fuhrmann and J. Salbeck, *Org. Electron.*, 2003, **4**, 61.
21 Z. Jiang, H. Yao, Z. Zhang, C. Yang, Z. Liu, Y. Tao, J. Qin and D. Ma, *Org. Lett.*, 2009, **11**, 2607.
22 Z. Jiang, Z. Liu, C. Yang, C. Zhong, J. Qin, G. Yu and Y. Yiu, *Adv. Funct. Mater.*, 2009, **19**, 3987.
23 S. Ku, W. Hung, C. Chen, S. Yang, E. Mondal, Y. Chi and K. Wong, *Chem.–Asian J.*, 2012, **7**, 133.
24 L. Chi, W. Hung, H. Chiu and K. Wong, *Chem. Commun.*, 2009, 3892.
25 T. Hwu, T. Tsai, W. Hung, S. Chang, Y. Chi, M. Chen, C. Wu, K. Wong and L. Chi, *Chem. Commun.*, 2008, 4956.
26 Y. Liao, C. Lin, Y. Liu, K. Wong, W. Hung and W. Chen, *Chem. Commun.*, 2007, 1831.
27 M. J. Frisch, G. W. Trucks, H. B. Schlegel, G. E. Scuseria, M. A. Robb, J. R. Cheeseman, J. A. Montgomery, T. Vreven, Jr, K. N. Kudin, J. C. Burant, J. M. Millam, S. S. Iyengar, J. Tomasi, V. Barone, B. Mennucci, M. Cossi, G. Scalmani, N. Rega, G. A. Petersson, H. Nakatsuji, M. Hada, M. Ehara, K. Toyota, R. Fukuda, J. Hasegawa, M. Ishida, T. Nakajima, Y. Honda, O. Kitao, H. Nakai, M. Klene, X. Li, J. E. Knox, H. P. Hratchian, J. B. Cross, C. Adamo, J. Jaramillo, R. Gomperts, R. E. Stratmann, O. Yazyev, A. J. Austin, R. Cammi, C. Pomelli, J. W. Ochterski, P. Y. Ayala, K. Morokuma, G. A. Voth, P. Salvador, J. J. Dannenberg, V. G. Zakrzewski, S. Dapprich, A. D. Daniels, M. C. Strain, O. Farkas, D. K. Malick, A. D. Rabuck, K. Raghavachari, J. B. Foresman, J. V. Ortiz, Q. Cui, A. G. Baboul, S. Clifford, J. Cioslowski, B. B. Stefanov, G. Liu, A. Liashenko, P. Piskorz, I. Komaromi, R. L. Martin, D. J. Fox, T. Keith, M. A. Al-Laham, C. Y. Peng, A. Nanayakkara, M. Challacombe, P. M. W. Gill, B. Johnson, W. Chen, M. W. Wong, C. Gonzalez and J. A. Pople, *Gaussian 03, revision B05*, Gaussian, Inc., Pittsburgh, PA, 2003.